PHYSICAL REVIEW E **76**, 045202(R) (2007)

Negative filament tension of scroll rings in an excitable system

Tamás Bánsági, Jr. and Oliver Steinbock*
Department of Chemistry and Biochemistry, Florida State University, Tallahassee, Florida 32306-4390, USA
(Received 12 July 2007; published 12 October 2007)

Scroll rings are three-dimensional spiral waves of excitation that rotate around circular filaments. In a modified Belousov-Zhabotinsky reaction, these filaments expand, buckle, and build up gradients in rotation phase. The instability is caused by negative filament tension (-4.3×10^{-4} cm^2/s). Initial deformations are strongest in the direction normal to the filament's osculating plane, and their growth rates decrease rapidly with increasing wave number.

DOI: 10.1103/PhysRevE.76.045202 PACS number(s): 05.45.−a, 82.40.Ck, 87.18.Pj

Numerous chemical and biological systems show topological defects that organize rotating spiral waves [1]. These excitation structures share intriguing similarities with vortices found in superfluids, superconductors, Bose-Einstein condensates, and nonlinear optical systems [2–4]. In all of these examples, vortex line motion is of particular interest as it affects vortex lifetimes and possible transitions into turbulent states. Moreover, spiral waves in excitable systems also have profound biological and medical relevance [5,6]. For instance, rotating concentration waves organize the aggregation of cellular slime molds [7] and vortical depolarization pulses induce debilitating or fatal arrhythmia in the human heart [8].

In spatially two-dimensional excitable media, spiral waves rotate around a nearly quiescent core region. Accordingly, the rotation of scroll waves, the three-dimensional analogs of spirals, occurs around tubular regions which are well represented by one-dimensional space curves. These filaments are boundary- or wave-terminated lines, closed rings, chains, and knots [9]. In general, filaments are not stationary but move, stretch, and bend according to their shape, phase gradients in spiral rotation ("twist"), and system-specific parameters [10].

Of particular interest is the question of whether untwisted, circular filaments expand or collapse. Experimental studies, all of which employed the Belousov-Zhabotinsky (BZ) reaction, revealed that such scroll rings shrink, drift, and eventually self-annihilate [11,12]. Overall, these experimental results are in agreement with predictions based on the equations

$$\frac{dR}{dt} = -\frac{\alpha}{R}, \quad \frac{dz}{dt} = \frac{\beta}{R}, \tag{1}$$

where t, R, and z denote time, the filament radius, and the spatial coordinate normal to the filament, respectively. In all experiments, the filament tension α and the drift parameter β were reported to be positive quantities.

Nonetheless, for two decades theoretical studies have predicted the possibility of scroll ring expansion ($\alpha<0$) [13]. This negative filament tension (NT) has also been tied to an instability that results in NT (or Winfree) turbulence [14]. The latter state is qualitatively different from chaotic dynamics induced by spiral core breakup or far-field breakup [15] and does not exist in two-dimensional systems. Moreover, onset of NT turbulence has been linked to the deterioration of cardiac tachycardia to ventricular fibrillation, with the latter being among the most common causes of death in the industrialized world [16]. It is, hence, not surprising that the study of negative filament tension in scroll waves has attracted considerable interest among physicists. However, no experimental observations of NT scroll rings have been reported to date. In this Rapid Communication, we document the existence of NT scroll rings in a chemical reaction-diffusion system. Using these observations, we also determine the parameters α and β and characterize the onset of buckling.

Our experiments utilize an excitable BZ medium in which the classic organic substrate as well as the catalyst are replaced by 1,4-cyclohexanedione (CHD) and $Fe[batho(SO_3)_2]_3^{4-}$, respectively, where batho deontes 4,7-diphenyl-1, 10-phenanthroline. The first substitution excludes gas-forming reactions that would otherwise nucleate undesired bubbles, while the latter substitution yields a conveniently large difference between the extinction coefficients of the reduced and oxidized catalyst species. The reaction system is prepared from stock solutions of CHD (Aldrich), $NaBrO_3$ (Fluka), H_2SO_4 (Riedel–de Haën), and the catalyst as well as nanopure water and polyacrylamide solution. The latter compound increases the viscosity of the BZ solution from about 1 to 150 mPa s and suppresses undesired convection. The preparation of the catalyst and the polyacrylamide solution is described in Ref. [17]. All measurements employ a cylindrical glass cuvette (inner diameter 3.7 cm) and are carried out at a temperature of 21 ± 1 °C. Notice that after mixing of all reagents the system is initially unexcitable for about 80 min.

Waves are monitored and reconstructed using optical tomography as described by Winfree and others [18]. For this purpose, the sample is rotated at a constant period of 4.9 s around its symmetry, or z, axis. Using a charge-coupled-device camera, transmission images of the illuminated, rotating sample are recorded at a rate of 12.5 frames/s, which corresponds to 62 projections per full rotation. From these data, we extract a sinogram for each z value. Using filtered back projection, every sinogram yields the reconstructed absorption fields at the given height z and, by repetition, the

*steinbck@chem.fsu.edu

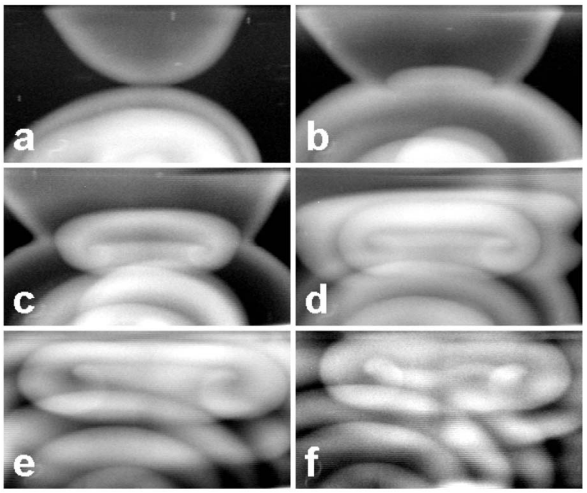

FIG. 1. Snapshots of the formation and subsequent dynamics of an initially axisymmetric scroll ring in a three-dimensional 1,4-cyclohexanedione Belousov-Zhabotinsky (CHD BZ) system. Reactant concentrations: $[H_2SO_4]=0.6$ mol/L, $[NaBrO_3]=0.175$ mol/L, [CHD]=0.2 mol/L, and $[Fe[batho(SO_3)_2]_3^{4-}]=0.475$ mmol/L. Time elapsed between snapshots: 45, 33, 40, 131, and 111 s. Area of each transmission image: 14.7×8.1 mm^2.

desired three-dimensional reconstruction of the wave pattern.

Rotating scroll rings are initiated using a technique described earlier [12]. It exploits the anomalous dispersion of the CHD BZ reaction, which has been described and analyzed in Ref. [19]. For the given reactant concentrations, this so-called anomaly yields fast-moving waves in the wake of a slow, leading pulse. The latter situation induces front-to-back collisions in which the trailing excitation pulses disappear. These dynamics are called "wave merging" and have been observed not only in the CHD BZ reaction but also during catalytic surface processes [20] and in generic models of reaction-diffusion media [21].

Figure 1 shows a sequence of six snapshots obtained at a constant angle of observation. Dark areas correspond to chemically reduced and dynamically excitable regions, while the oxidation waves appear as bright bands. Notice that these snapshots are views through a thick, three-dimensional medium. Hence, multiple waves can exist at different depths, causing the incorrect impression of interference phenomena. The first three snapshots in Fig. 1 illustrate the specific initiation process of the rotating scroll ring. This process requires three circular wave fronts, which we trigger from small silver particles and wires that locally decrease the concentration of the inhibitor bromide. The two outermost waves collide and create an hourglass-shaped wave structure with an "equatorial hole" [Figs. 1(a) and 1(b)]. The two lower waves undergo a front-to-back collision in which the trailing wave disappears. However, within the equatorial region a small segment survives the latter collision [Fig. 1(b)] and nucleates an untwisted, axisymmetric scroll ring [Fig. 1(c)].

Figures 1(d)–1(f) are a representative example for the subsequent dynamics of scroll rings in this system. A comparision of Figs. 1(c)–1(e) shows that the scroll ring expands and moves upward. The snapshots Figs. 1(e) and 1(f) reveal the emergence of phase gradients in spiral rotation, which twist the initially axisymmetric vortex. In addition, the initially planar rotation backbone undergoes deformations which create the impression of an undulated structure in the upper half of Fig. 1(f).

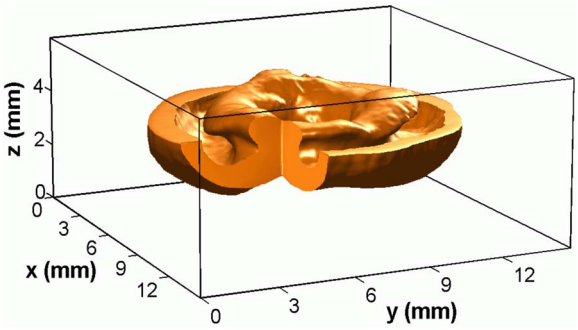

FIG. 2. (Color online) Reconstruction of a three-dimensional scroll ring using optical tomography. The reconstruction is based on data from the experiment shown in Fig. 1.

Using the methods described above, we can reconstruct the full three-dimensional absorption data associated with a wave structure at different times. Figure 2 shows a typical example that corresponds to the projection in Fig. 1(f). In the tomographic reconstruction, nonexcited regions are transparent while excitation waves are visualized as solid objects. To reveal details of the pattern, we omitted all waves that are more than approximately one vortex pitch away from the filament and also removed a box-shaped section in the foreground. Overall, Fig. 2 clearly illustrates the spiral structure of the excitation vortex. Furthermore, one can discern the filament and its deviations from a perfect circle as the undulated rim in the central portion of the viewing box.

From data similar to those shown in Fig. 2, three-dimensional curves are extracted that represent the vortex filaments at various times. This analysis employs two-

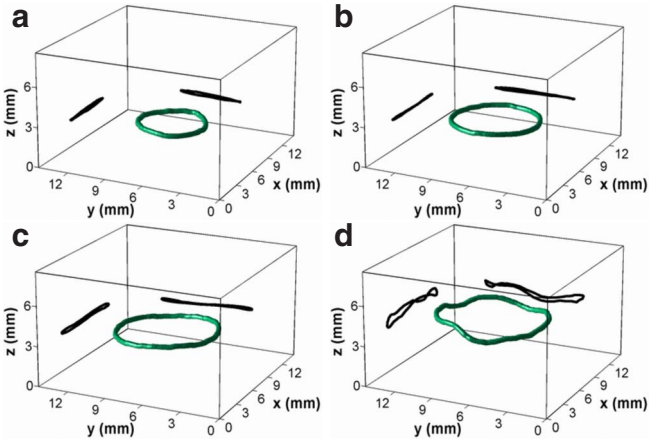

FIG. 3. (Color online) Three-dimensional reconstruction of an expanding and buckling scroll ring filament along with corresponding two-dimensional projections. (a)–(d) depict the filament at times 0, 73, 119, and 315 s, respectively. All experimental parameters as stated in Fig. 1.

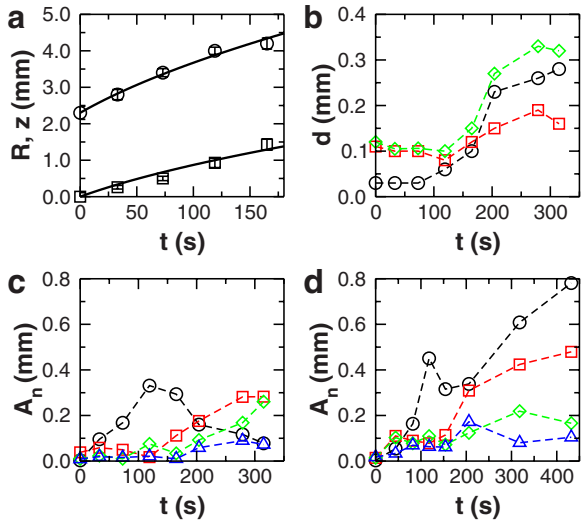

FIG. 4. (Color online) (a) Temporal evolution of the radius (circles) and the vertical coordinate (squares) of an expanding scroll ring filament. The solid lines are fits based on the solutions of Eqs. (1). (b) Time dependence of the root-mean-square distance between the buckling filament and its best-fit circles (diamonds). The corresponding root-mean-square values of the radial and normal components are shown as squares and circles, respectively. (c), (d) Time dependencies of the Fourier amplitudes $n=1$ (circles), 2 (squares), 3 (diamonds), and 4 (triangles) for the filaments of a small and a large scroll ring, respectively.

dimensional, planar cross sections in which the filament position is measured as the location of spiral tips. Figure 3 shows a sequence of three-dimensional graphs describing the evolution of a scroll ring filament. The data show that the initially circular filament is expanding while maintaining a nearly planar geometry. As clearly discernible in Fig. 3(d), this expansion is followed by a loss of planarity. Reliable analyses of the subsequent dynamics are severely hindered by the increasing number of wave pulses and hence are not presented.

To further quantify the expansion and buckling dynamics, we measure the mean filament radius R and the mean filament position in the vertical direction z as functions of time t. We consider only the first 165 s of scroll wave dynamics, during which the filament remains nearly circular. These data are shown in Fig. 4(a) along with least-squares fits based on the solutions of Eqs. (1): $R(t)=\sqrt{R_0^2-2\alpha t}$ and $z(t)=z_0-\beta R(t)/\alpha$, where R_0 is the filament radius at $t=0$ and $z_0=\beta R_0/\alpha$. The fit for $R(t)$ is in very good agreement with our measurements and yields a filament tension of $\alpha=-(4.3\pm0.2)\times10^{-4}$ cm^2/s. To our knowledge this is the first experimental observation of negative filament tension in excitable systems. The fit for $z(t)$ is satisfactory and yields a drift parameter of $\beta=(2.6\pm0.2)\times10^{-4}$ cm^2/s. However, our R data show a much better square root dependence than the latter, vertical coordinates. We note that a similar deviation has been found in numerical simulations of reaction-diffusion models [22].

Figure 4(b) quantifies the onset of buckling in terms of the distance between the actual filament and its best-fit circle. Our least-squares fitting procedure allows for tilted circles and yields distance vectors as a function of the azimuth ϕ. In Fig. 4(b), open squares and circles represent the root-mean square distances $\langle d_r\rangle$ and $\langle d_\perp\rangle$ in the radial and normal directions to the filament plane, respectively. Open diamonds correspond to the root-mean square of the total distances. The data show that NT-induced buckling in the z direction is stronger than deformations within the filament plane. For example, over the duration of the analyzed time interval (315 s), $\langle d_r\rangle$ increases by merely 50%, while $\langle d_\perp\rangle$ increases by 800%. This effect can only be caused by the curvature of the filament. As a general conclusion, the latter finding implies that NT-induced filament deformations are reduced within the filament's osculating plane. Furthermore, it seems likely that the extent of this stabilization increases monotonically for increasing values of the local curvature. These conclusions are supported by experiments with larger scroll rings (not shown), for which we detect smaller differences between $\langle d_r\rangle$ and $\langle d_\perp\rangle$.

Further inspection of the data in Fig. 4(b) also suggests that the buckling instability is either absent or very weak during the first 150 s. This observation prompted us to carry out a time-resolved mode analysis of buckling filaments. For this purpose, the filament deviations $d_\perp(\phi)$ are recalculated with respect to the orientation of the *earliest* set of filament coordinates, and their Fourier transforms are computed. Figures 4(c) and 4(d) show the time-dependent Fourier amplitudes A_n for the modes $n=1-4$ as obtained from two independent experiments. More specifically, the results in Fig. 4(c) are from the same experiment that we analyzed for Figs. 4(a) and 4(b), while Fig. 4(d) describes the buckling of an initially two-times larger scroll ring filament ($R_0=4.7$ mm). Notice that (i) the expansion of the latter filament is slower than the growth of the smaller one [cf. Eqs. (1)], (ii) the mode $n=1$ is mainly a tilt of the filament away from its original orientation and, hence, is not fully captured by the analysis in Fig. 4(b), and (iii) that the wave number $k=n/R(t)$ of a given mode decreases in the course of scroll ring expansion.

Over the duration of both experimental runs, the deformation amplitudes A_n remain very low for modes with $n\geq5$ (not shown). Figures 4(c) and 4(d) clearly show that the amplitudes of modes $n=1-4$ increase in time. Only A_1 in Fig. 4(c) decreases after an initially rapid increase. Furthermore, we find overall higher amplitudes for the larger scroll ring. This finding agrees well with the visual impression that large scroll rings buckle faster and more strongly than smaller ones. More importantly, we find that, in both examples, the growth rates of the first four modes decrease with increasing n.

The latter result can be discussed in the context of results by Henry and Hakim [23], who carried out a linear stability analysis of scroll waves rotating around a straight filament. For NT conditions, such rotors can be unstable against perturbations in the z direction. The corresponding growth rates $\sigma(k_z)$ are negative (i.e., stable) for large wave numbers and positive (unstable) in a finite band between zero and a unique critical value k_{crit}. Within this band, growth rates have a single maximum at k_{max}, and converge to zero for small k_z.

These results should also apply to very large scroll rings and hold at least qualitatively for smaller ones if the rate of filament expansion is small compared to the growth rates of filament deformations. Therefore, we can interpret the observed decrease in growth rates with increasing n [Figs. 4(c) and 4(d)] as wave numbers between k_{max} and k_{crit} where $d\sigma/dk<0$. Accordingly, NT scroll rings larger than the ones studied here should show a nonmonotonic dependence of growth rates on n. Moreover, we can explain the absence of deformations for large n values as deformations with $k>k_{crit}$. This interpretation yields $k_{crit}\approx 1$ mm^{-1} as a rough estimate for scroll rings in this specific chemical system.

For very small scroll rings ($R\lesssim 1/k_{crit}$), however, quantization effects have to be considered because a circular filament can be too short to accommodate potentially unstable modes of large wavelength. We suggest that the very slow, possibly delayed, growth of modes with $n>1$ in Fig. 4(c) could possibly be a consequence of this quantization-induced stabilization. Clearly more experimental as well as theoretical studies are needed to address this feature of NT scroll rings. Future experimental work should also include the measurement of $\sigma(k_z)$ and its radius dependence. Moreover, it will be interesting to study the nonlinear stages of NT dynamics and attempt to characterize NT turbulence experimentally.

This material is based upon work supported by the National Science Foundation under Grant No. 0513912.

[1] M. C. Cross and P. C. Hohenberg, Rev. Mod. Phys. **65**, 851 (1993); C. Walgraef, *Spatio-Temporal Pattern Formation (With Examples from Physics, Chemistry, and Materials Science)* (Springer Verlag, New York, 1997).
[2] M. R. Matthews, B. P. Anderson, P. C. Haljan, D. S. Hall, C. E. Wieman, and E. A. Cornell, Phys. Rev. Lett. **83**, 2498 (1999).
[3] J. Leach, M. R. Dennis, J. Courtial, and M. J. Padgett, New J. Phys. **7**, 55 (2005).
[4] I. S. Aranson and L. Kramer, Rev. Mod. Phys. **74**, 99 (2002).
[5] A. Goldbeter, *Biochemical Oscillations and Cellular Rhythms* (Cambridge University Press, Cambridge, U.K. 1996).
[6] F. H. Fenton, E. M. Cherry, A. Karma, and W. J. Rappel, Chaos **15**, 013502 (2005).
[7] O. Steinbock, F. Siegert, S. C. Müller, and C. Weijer, Proc. Natl. Acad. Sci. U.S.A., USA **90**, 7332 (1993).
[8] F. X. Witkowski, L. J. Leon, P. A. Penkoske, W. R. Giles, M. L. Spano, W. L. Ditto, and A. T. Winfree, Nature (London) **392**, 78 (1998); J. M. Davidenko, A. V. Pertsov, R. Salomonsz, W. Baxter, and J. Jalife, *ibid.* **355**, 349 (1992).
[9] P. M. Sutcliffe and A. T. Winfree, Phys. Rev. E **68**, 016218 (2003); T. Bánsági Jr., C. Palczewski, and O. Steinbock, J. Phys. Chem. A **111**, 2492 (2007).
[10] J. P. Keener, Physica D **31**, 269 (1988); B. Echebarria, V. Hakim, and H. Henry, Phys. Rev. Lett. **96**, 098301 (2006).
[11] M. Vinson, S. Mironov, S. Mulvey, and A. Pertsov, Nature (London) **386**, 477 (1997).
[12] T. Bánsági Jr. and O. Steinbock, Phys. Rev. Lett. **97**, 198301 (2006).
[13] A. V. Panfilov and A. N. Rudenko, Physica D **28**, 215 (1987).
[14] S. Alonso, F. Sagues, and A. S. Mikhailov, Science **299**, 1722 (2003); R. M. Zaritski, S. F. Mironov, and A. M. Pertsov, Phys. Rev. Lett. **92**, 168302 (2004).
[15] M. Bär and L. Brusch, New J. Phys. **6**, 5 (2004).
[16] S. Alonso and A. V. Panfilov, Chaos **17**, 015102 (2007).
[17] N. Manz, B. T. Ginn, and O. Steinbock, J. Phys. Chem. A **107**, 11008 (2003); T. Rica, D. Horváth, and Á. Tóth, Chem. Phys. Lett. **408**, 422 (2005).
[18] A. T. Winfree, S. Caudle, G. Chen, P. McGuire, and Z. Szilagyi, Chaos **6**, 617 (1996); U. Storb, C. R. Neto, M. Bär, and S. C. Müller, Phys. Chem. Chem. Phys. **5**, 2344 (2003).
[19] C. T. Hamik, N. Manz, and O. Steinbock, J. Phys. Chem. A **105**, 6144 (2001).
[20] J. Christoph, M. Eiswirth, N. Hartmann, R. Imbihl, I. Kevrekidis, and M. Bär, Phys. Rev. Lett. **82**, 1586 (1999).
[21] N. Manz, C. T. Hamik, and O. Steinbock, Phys. Rev. Lett. **92**, 248301 (2004).
[22] See, e.g., Fig. 5 in S. Alonso and A. V. Panfilov, Chaos **17**, 015102 (2007).
[23] H. Henry and V. Hakim, Phys. Rev. Lett. **85**, 5328 (2000); Phys. Rev. E **65**, 046235 (2002).